8.07f/W(Jul162004)
+model
JNDT : 908
Prod.Type:FTP
pp.1–5(col.fig.:NIL)
ED:SreejaGA
PAGN:Bhaskara SCAN:

ARTICLE IN PRESS

Available online at www.sciencedirect.com
ScienceDirect

ELSEVIER

NDT&E International ▮ (▮▮▮▮) ▮▮▮–▮▮▮

NDT&E international

www.elsevier.com/locate/ndteint

Flaw detection in metals by the ACPD technique: Theory and experiments

H. Saguy, D. Rittel*

Faculty of Mechanical Engineering, Technion, 32000 Haifa, Israel

Received 5 February 2007; accepted 13 April 2007

Abstract

The Alternating Crack Potential Drop (ACPD) technique is mainly used to characterize surface cracks in metals. To-date, this technique has the following two limitations: it is limited to the so-called thin skin assumptions, and is applicable to open (visible) flaws. Saguy and Rittel recently proposed a methodology based on numerical simulations to overcome these limitations [Saguy H, Rittel D. Bridiging thin and thick skin solutions for alternating currents in crack conductors. Appl Phys Lett J 2005; 87: 84103–84103/3; Saguy H, Rittel D. Alternating current flow in internally flawed conductors: a tomographic analysis. Appl Phys Lett J 2006; 89: 94102–94102/3]. This paper presents experimental results, which support the proposed solutions and methodology to expand the universality of the ACPD technique as a key NDT tool.

Keywords: ACPD; Surface flaw; Hidden flaw; NDT.

1. Introduction

Alternating Crack Potential Drop (ACPD) is a non-destructive testing technique, which is mainly used to estimate surface flaws in metals [1,2]. The technique is based on the skin effect phenomenon [3–6]. When an AC current flows through a metallic conductor, the current is constrained to a skin whose thickness δ depends on the current frequency f, and the conductor's physical properties:

$$\delta = \frac{1}{(\pi \mu_r \mu_0 \sigma f)^{1/2}}, \quad (1)$$

where μ_r is the relative magnetic permeability, μ_0 the magnetic permeability of free space measured and σ the electrical conductivity.

The spatially limited flow of AC currents can be exploited to detect and measure the size of surface open flaws in the so-called ACPD technique. In the ACPD technique, an AC current is injected at point 1 and flows along the metal surface, down and up the flaw, and out through point 2 (Fig. 1). The current concentrates into a thin skin of thickness δ. The skin circumvents a flaw of a uniform depth d. The voltage drop is measured by a probe with fixed gap, Δ, between its electrodes. A reference voltage V_1 is measured far from the crack, and V_2 is measured across the crack flanks.

The voltage ratio V_2/V_1 is translated into flaw depth either by a theoretical approximation or by means of a calibration procedure.

Two modes of current flow are identified, namely the thin and thick skin modes [3,7,8]. Each mode depends on the flaw dimensions (d, L), current frequency (f) and the probe (through the distance between the electrodes-Δ). The thin skin approximation for crack depth estimation is well established and supported experimentally [3,7,8].

When thin skin conditions are met, the crack depth is approximated by

$$d = \frac{\Delta}{2}\left(\frac{V_2}{V_1} - 1\right). \quad (2)$$

Eqn. (2) is referred to as the *one-dimensional* (*1D*) *approximation* of the crack depth and it gives an excellent

*Corresponding author.
E-mail address: merittel@technion.ac.il (D. Rittel).

0963-8695/$ - see front matter © 2007 Elsevier Ltd. All rights reserved.
doi:10.1016/j.ndteint.2007.04.003

Please cite this article as: Saguy H, Rittel D. Flaw detection in metals by the ACPD technique: Theory and experiments. NDT&E Int (2007), doi:10.1016/j.ndteint.2007.04.003

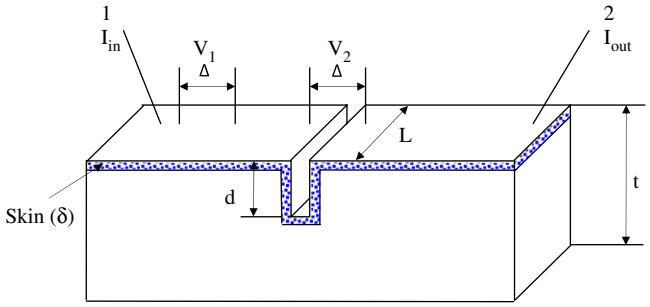

Fig. 1. A schematic description of the ACPD technique—surface flaw.

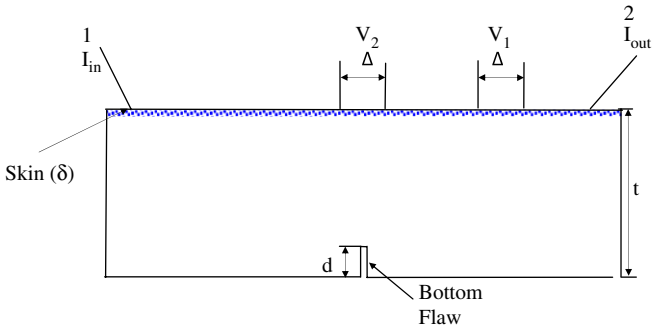

Fig. 2. Schematic description of the ACPD Technique—bottom flaw.

prediction of the crack depth *provided all the conditions of thin skin are met*.

The thick skin solution is a modification (or rather an adjustment) of the thin skin solution that requires cumbersome experimental calibration.

For a thick skin, an approximation of the flaw depth is given by [9–11]

$$d = \frac{\Delta}{2}\left(\frac{V_1}{V_2}\right)^{1/2}\left(\frac{V_2}{V_1} - 1\right). \tag{3}$$

This approximation gives a lower limit of the crack depth and is not a tight estimation. Saguy and Rittel proposed a *seamless transition between the thin- and the thick skin approximations*, which would allow a systematic variation of the experimental parameters [1]. Their main results can be summarized by the following equation:

$$\frac{V_2}{V_1} = \frac{\Delta + 2d - f_1(\Delta,\delta) - f_2(d,\delta)}{\Delta}, \tag{4}$$

where the functions f_1 and f_2 represent the "corner effect" for current flow around the flaw. Therefore, f_1 and $f_2$are dominant for the thick skin and negligible for the thin skin. The function f_1 compensates for the decrease of the voltage on the specimen surface and is dependent on Δ and δ. The function f_2 compensates for the decrease of the voltage on the crack plane and is, therefore, dependent on both d and δ.

The proposed empirical equations, which include the corner effect, are thus given by [1]

$$f_1(\Delta,\delta) = \Delta\,\exp\left(-\frac{(\Delta/2)+\delta}{\delta}\right), \tag{5}$$

$$f_2(d,\delta) = 2d\,\exp\left(-\frac{d+\delta}{\delta}\right). \tag{6}$$

Eq. (4) has the practical advantage that it *lifts the thin skin restriction*, thus allowing for crack sizing irrespective of the material, flaw and structure dimensions.

Another important progress concerns the assessment of hidden flaws, e.g. *bottom breaking* and *internal cracks* using the ACPD technique [2].

Fig. 2 is a schematic representation of the uniform current flow within a skin of thickness δ, in a conductor that contains bottom crack of uniform depth d. The current is injected at point 1, flows along the metal surface and exits at point 2. The voltage drop is measured by a probe whose contacts form a constant gap Δ. When placing the probe far away from the crack, a voltage V_1 is measured (reference voltage). A voltage V_2 is measured when placing the probe across the bottom crack.

The proposed methodology is based on changing the frequency systematically and measuring the voltage ratio. The numerical work shows that when the ratio between the skin thickness and the uncracked depth $\delta/(t-d)$ is small, the voltage ratio V_2/V_1 is constant (and equal to 1). It was found that when $\delta/(t-d) > 0.5$, a *universal drop* in the voltages ratio can be observed, so that the flaw depth can be found in a straightforward manner from:

$$\frac{\delta}{(t-d)} = 0.5. \tag{7}$$

The results described in the introductory section were obtained by means of numerical (finite element) simulations of current flow in flawed conductors. For all practical purposes, it is important to have an experimental support for the basic results to assess the limits of applicability of the proposed methodology. Experimental validation of the proposed methodology is precisely the concern of this paper.

2. Experimental procedure

2.1. Specimens and materials

Two types of problems were examined: surface and bottom notches with uniform depth. The notches studied in this work are sharp, yet they are to be considered as notches in the sense that a clear discontinuity is created without partial contact between actual crack flanks. Various frequencies were used in order to model thin- and thick skin conditions. The material and geometrical characteristics are listed in Table 1.

2.2. The experiments

The measurements were carried out using an AC signal generator, power amplifier (operated as a constant current operational amplifier at frequencies 5–20 KHz), probes

Please cite this article as: Saguy H, Rittel D. Flaw detection in metals by the ACPD technique: Theory and experiments. NDT&E Int (2007), doi:10.1016/j.ndteint.2007.04.003

Table 1
Materials and geometrical details of the specimens

Spec. No.	Notch type	Material	Length (mm)	Width (mm)	Thickness (mm)	Notch depth (mm)
1–4	Surface notch—uniform depth	AISI 1020—steel	200	50	25	1,3,5,8
5–7	Surface notch—uniform depth	SAE 304 L—stainless steel	200	50	25	3,5,8
8	Surface notch—uniform depth	Al6061—aluminum alloy	200	50	25	8
9	Bottom notch—uniform depth	SAE 304 L—stainless steel	200	50	20	12

(homemade), voltage amplifier, and a digital oscilloscope. The system was set to the following specifications:

Generated current $I =$ 0.5–2 A.
Frequency: 5–20 kHz.
Voltage amplifiers gain: 80 db.
Distance between the probes (fixed): $\Delta = 10$ mm.

A constant current of 0.5–2 A was supplied to the specimens. The current was connected through screwed connections at the upper ends of the specimens. Each specimen contained a single notch so that the distance between the current input point and the crack was large enough (>100 mm) to achieve a uniform field in the crack area,. Two measurements of the voltage were taken at each frequency: one across the crack V_2, and the other far away from it (V_1 reference value). The voltage measurements V_1 and V_2 were then inserted into Eqs. (2)–(4) and notch depth was calculated accordingly. The probe was homemade of two spring-loaded copper needles, 1 mm in diameter. The probe's wires were twisted together once they left the specimen surface to maintain a minimum loop area, thus reducing stray noises.

2.3. Experimental results

2.3.1. Surface notch

In order to examine the validity of the proposed equation (Eq. (4)) on different materials, the following 3 materials were tested: AISI 1020 steel, SAE 304L stainless steel and Al6061 aluminum alloy (Table 1).

Figs. 3–5 show a comparison of the predicted notch depth for specimens with a surface notch between the 1D approximation (Eq. (2)), thick equation (Eq. (3)) and proposed equation (Eq. (4)) (based on the experimental results).

Fig. 3 shows a comparison for AISI 1020 steel specimens with 1, 3, 5 and 8 mm uniform notch depth (specimens 1–4, Table 1), for which all the tests were carried out in the *thin skin regime* (the skin thickness for steel at frequency 5–20 kHz is about 0.2–0.1 mm—i.e. very small compared with the thickness and the notch).

Fig. 3 shows an excellent agreement between the 1D approximation (Eq. (2)), the proposed equation (Eq. (4)) and the actual notch depth. As expected, when all the conditions for a thin skin are met, the proposed equation (Eq. (4)) and the 1D approximation (Eq. (2)) give identical values of the notch depth, since the corner effect is negligible [2]. In this case, the voltage ratio depends only on the probe distance (Δ) and the crack depth (d) (Eq. (2)). This explains why the predicted notch depth shown in Fig. 3 is constant and does not depend on the skin thickness (δ).

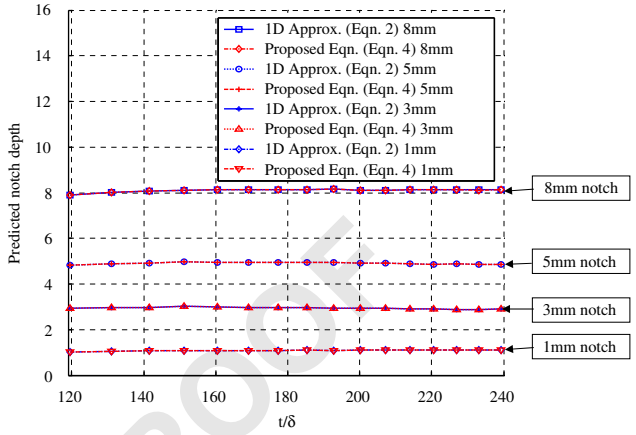

Fig. 3. Predicted notch depth vs. t/δ for steel specimens with uniform depth surface notch.

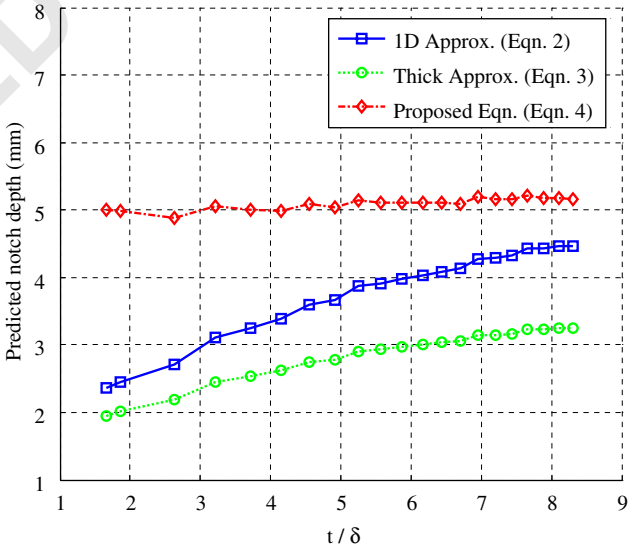

Fig. 4. Predicted notch depth vs. t/δ at stainless steel specimen with uniform depth surface notch of 5 mm.

The maximum measured error in notch depth is 11% for the 1 mm notch and less then 4% for all other notches (3, 5 and 8 mm).

Fig. 4 shows results for 304L stainless steel specimens with 5 mm uniform notch depth (specimen 6, Table 1).

Please cite this article as: Saguy H, Rittel D. Flaw detection in metals by the ACPD technique: Theory and experiments. NDT&E Int (2007), doi:10.1016/j.ndteint.2007.04.003

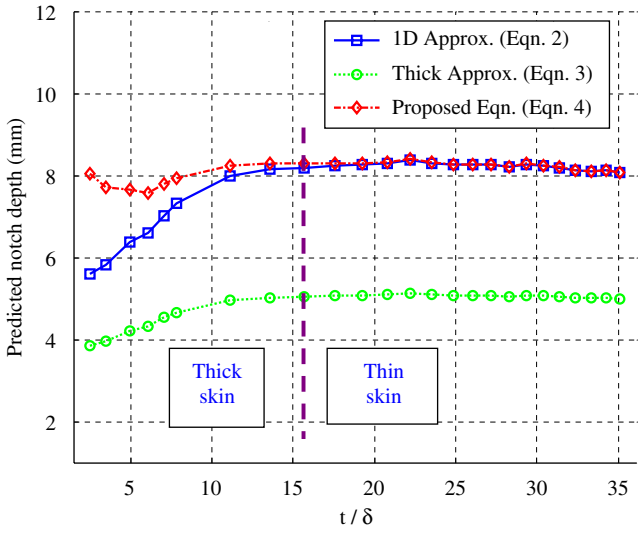

Fig. 5. Predicted notch depth vs. t/δ for aluminum specimen with 8 mm uniform depth surface notch.

Here, all the measurements were carried out in the *thick skin regime* (the skin thickness for stainless steel at frequency 5–20 kHz is about 6–3 mm).

In this case, there is an excellent agreement between the proposed equation (Eq. (4)) and the actual notch depth (5 mm). As expected, the 1D approximation (Eq. (2)) and the thick approximation (Eq. (3)) do not provide a good estimate of the notch depth, and the error increases as the skin thickness (δ) increases (because the corner effect increases).

The proposed equation gives a maximum measured error in notch depth that is less than 5%. The maximum measured error is 53% for the 1D approximation and 61% for the thick approximation.

Finally, Fig. 5 shows a comparison for a 6061 aluminum alloy specimen (specimen 8, Table 1) subject *partly to thin skin and partly to thick skin conditions* (the skin thickness for aluminum at frequency 5–20 kHz is about 1.4–0.7 mm). Fig. 5 shows an excellent match between the proposed equation (Eq. (4)) and the actual notch depth (8 mm) at all frequencies (thin and thick skin regimes), whereas the 1D approximation (Eq. (4)) does not provide accurate results in the thick skin regime (left to the dashed line). Again, since the 1D approximation gives constant value at all frequency, the error increases as the skin thickness (δ) increases (the current frequency decreases).

The maximum measured error of the proposed equation is 5% of the notch depth. A maximum error of 30% results for the 1D approximation and 52% for the thick approximation.

2.3.2. Hidden (bottom) notch

Fig. 6 shows a comparison between the experimental and numerical results for a stainless steel specimen with uniform depth bottom notch (specimen number 9, Table 1). In this case, the notch depth (d) is 12 mm, the specimen

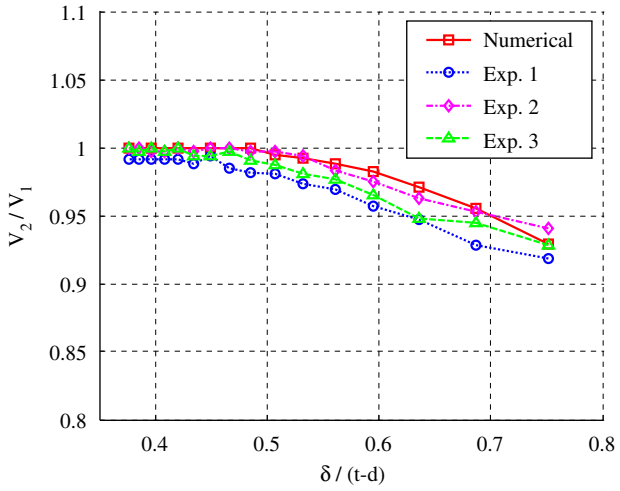

Fig. 6. A comparison between the experimental and numerical results for stainless steel specimen with uniform depth bottom notch (specimen 9, Table 1).

thickness (t) is 20 mm, and the uncracked depth ($t-d$) is 8 mm. According to the numerical results [2], it is expected that as long as $\delta/(t-d) \leqslant 0.5$, the electrical field is not affected by the presence of the bottom crack and the ratio V_2/V_1 should remain constant and equal to 1. Fig. 6 shows 3 sets of experimental results. The change in the voltage ratio is indeed observed at $0.46 < \delta/t-d < 0.53$, which is in remarkable agreement with the numerical predictions. From Eq. (7), the notch depth (d) can be calculated: 11.9–11.98 mm (instead of 12 mm). The maximum error in notch depth estimation is less then 1% (of the notch depth).

3. Discussion

The experimental work focused on confirming previous numerical modeling work providing a seamless bridge between *thin- and thick skin solutions for surface flaws*, and also on a novel methodology to *identify and size bottom (hidden) flaws.*

Experiments were carried out on specimens from 3 different materials (carbon steel, stainless steel and aluminum alloy) to replicate all possible skin configurations, namely thin, thick and mixed.

Fig. 3 shows that for the thin skin case, there is an excellent match between the 1D approximation (Eq. (2)), the proposed equation (Eq. (4)), and the actual notch depth at all frequencies. This result confirms the validity of the experimental setup as it addresses a thin skin mode for which an analytical solution is available, that has been thoroughly validated experimentally.

In contrast, thick skin and thin–thick skin combinations (Figs. 4 and 5) reveal an excellent match only between the proposed equation (Eq. (4)) and the actual notch depth at all frequencies, thus demonstrating the validity of Eq. (4) for any skin thickness situation. These results also illustrate the domain of applicability of the 1D approximation (Eq.

Please cite this article as: Saguy H, Rittel D. Flaw detection in metals by the ACPD technique: Theory and experiments. NDT&E Int (2007), doi:10.1016/j.ndteint.2007.04.003

(2)), as well as its limitations. It can thus be concluded that for thick skin conditions, the 1D approximation does not provide an accurate prediction of the notch depth, when compared with the global Eq. (4).

The applicability of ACPD technique to hidden flaws, of which bottom flaws as investigated here are a particular case, has not been extensively investigated. An important universal relation was predicted to tie the remote and local voltage ratio and the flaw depth (Eq. (7)). This simple equation answers the question of the existence of a flaw, and also provides its depth with a high degree of accuracy, as shown in Fig. 6.

The experiments shown here, together with their theoretical framework extend significantly the field of application of the ACPD technique.

4. Conclusion

New experimental results have been shown to be in excellent agreement with the theoretical results of Saguy and Rittel [1,2].

Namely, for various skin configurations, ranging from thin to thick through mixed-mode, surface flaw depth could be precisely determined without the limitation of 1D available solution.

Moreover, the issue of hidden flaws (bottom notch) was successfully addressed from an experimental point of view, showing that such flaws can be identified and their depth assessed using ACPD technique. The presented applications are deemed to significantly expand the range of applications of the ACPD technique.

References

[1] Saguy H, Rittel D. Bridging thin and thick skin solutions for alternating currents in crack conductors. Appl Phys Lett J 2005;87:84103–84103/3.

[2] Saguy H, Rittel D. Alternating current flow in internally flawed conductors: a tomographic analysis. Appl Phys Lett J 2006;89:94102–94102/3.

[3] Collins R. Dover WD, Michael DH. The use of AC field measurement for NDT, 1985; 8: 211–65.

[4] Collins R, Dover WD, Ranger KB. The AC field around a plane semi-elliptical crack in metal surface, 1981; 470–9.

[5] Dover WD, Collins R, Michael DH. Review of development in ACPD and ACFM. Br J NDT 1991;33(3):121–7.

[6] Johnson WC. The constants of two-conductor lines, 1950; 1: 58–80.

[7] Dover WD, Monahan CC. The measurement of surface breaking cracks by the electrical systems ACPD/ACFM. Fatigue Fract Eng 1994;17(12):1485–92.

[8] Dover WD, Charlesworth FDW, Taylor KA, Collins R, Michael DH. AC field measurement—theory and practice, 1980; 222–61.

[9] Lugg MC. Data interpretation in ACPD crack inspection. NDT Int 1989;22(3):149–54.

[10] Mirshekar-Syahkal D, Collins R, Michael DH. The influence of skin depth on crack measurement by the AC field technique. Nondestruct Eval 1982;3(2):65–76.

[11] Michael DH, Collins R. The AC field around a plane crack in metal surface when the skin depth is large. Nondestruct Eval 1982;3(1):19–24.

Please cite this article as: Saguy H, Rittel D. Flaw detection in metals by the ACPD technique: Theory and experiments. NDT&E Int (2007), doi:10.1016/j.ndteint.2007.04.003